

PAPER • OPEN ACCESS

## LCT, PIV and IR Imaging Detection in Selected Technical and Biomedical Applications

To cite this article: Jan Stasiek and Marcin Jewartowski 2019 *J. Phys.: Conf. Ser.* **1224** 012029

View the [article online](#) for updates and enhancements.



**IOP | ebooks™**

Bringing you innovative digital publishing with leading voices to create your essential collection of books in STEM research.

Start exploring the collection - download the first chapter of every title for free.

# LCT, PIV and IR Imaging Detection in Selected Technical and Biomedical Applications

**Jan Stasiek, Marcin Jewartowski**

Gdansk University of Technology, Faculty of Mechanical Engineering, Department of Energy and Industrial Apparatus, ul. G.Narutowicza 11/12, 80-233 Gdansk, Poland

jstasiek@pg.edu.pl

**Abstract.** Thermochromic liquid crystals (TLC), Particle Image Velocimetry (PIV) and Infrared Imaging Thermography (IR) have been successfully used in non-intrusive technical, industrial and biomedical studies and applications. These four tools (based on the desktop computers) have come together during the past two decades to produce a powerful advanced experimental technique as a judgment of quality of information that cannot be obtained from any other imaging procedure. The brief summary of the history of this technique is reviewed, principal methods and tools are described and some examples are presented. With this objective, a new experimental technique have been developed and applied to the study of heat and mass transfer and for biomedical diagnosis. Automated evaluation allows determining the heat and flow visualisation and locate the area of suspicious tissue of human body.

## 1. Introduction

In order to demonstrate the feasibility of thermochromic liquid crystals techniques, true-colour image processing, particle image velocimetry and infrared thermography in practical heat transfer, flow visualization and biomedical contexts several experiments has been performed. The first set was carried out to investigate temperature and then heat transfer coefficient distributions (in Nusselt number form) on film-heated models in channels with ribs/turbulators. Two experimental techniques were employed in the research for comparison: firstly, the steady-state and secondly transient technique. The flow pattern produced by transverse vortex generators (ribs) was visualized using planar beam of double-impulse laser tailored by a cylindrical lens and oil particles. Sequential images of the particles in a cross sectional plane taken with CCD video camera from the downstream side of the flow were stored on a personal computer to obtain distributions of velocity vectors by means of the PIV method.

Also in experimental investigation of the film cooling effectiveness for model turbine blades using TLC technique is presented. The film cooling and visualization of the few different holes configuration in steady-state and transient performance were analyzed experimentally.

In biomedical situations, e.g. skin diseases, breast cancer, blood circulation and other medical application, TLC, IR and image processing are successfully used as an additional non-invasive diagnostic method especially useful for screening large groups of potential patients. Biomedical data presented in the paper is based on results taken from literature and from medical researchers collaborating with authors. Most of described studies and obtained data (liquid crystals experiments, pressure gradient, flow visualization and PIV) provide useful information for better understanding of thermal performances of many industrial installations and medical examination.



## 2. Liquid Crystals

The original use of the term ‘liquid crystal’ is credited to Lehman, a German physicist, however they were first observed more than 130 years ago by an Austrian botanist, Friedrich Reinitzer [1]. In many publications of the time, Lehman use terms like Fliesende Krystalle (flowing crystals) and Flussige Krystalle (fluid crystals) to describe the unusual phase that existed between the two melting points of not only cholesteryl benzoate, but also a large number of other compounds he studied.

Liquid crystals are temperature indicators that modify incident white light and display colour whose wavelength is proportional to temperature. They can be painted on a surface or suspended in the fluid and used to make visible the distribution of temperature. Normally clear, or slightly milky in appearance, liquid crystals change in appearance over a narrow range of temperature called the ‘colour-play interval’ (the temperature interval between first red and last blue reflection), centered around the nominal ‘event temperature’. The displayed colour is red at the low temperature margin in the colour-play interval and blue at the high end. Within the colour-play interval, the colours change smoothly from red to blue as a function of temperature [2]. The effect is reversible which, in practical terms, means that a single application of liquid crystals to a model can be used repeatedly (usually until coating is obliterated or otherwise damaged). Both the colour play interval and the event temperature range of a liquid crystal can be selected by adjusting its composition, and materials are available with event temperatures from  $-30^{\circ}\text{C}$  to  $120^{\circ}\text{C}$  and with colour play bands from  $0.5^{\circ}\text{C}$  to  $20^{\circ}\text{C}$  [2-3] although not all combinations exist of event temperature and colour play band widths. Widths of  $1^{\circ}\text{C}$  or less will be called narrow band materials, while those whose band width exceeds  $5^{\circ}\text{C}$  will be called wide band. The types of material to be specified for a given task depend on the type of image interpretation technique to be used [4].

Liquid crystals are classified into three categories according to their molecular structures: smectic, nematic and cholesteric. However, from a structural viewpoint, it can be argued that there are only two basic types of liquid crystals, chiral-nematic and smectic, with cholesteric being regarded as a special kind of nematic. Some of their structures are shown schematically in figure 1 [5].

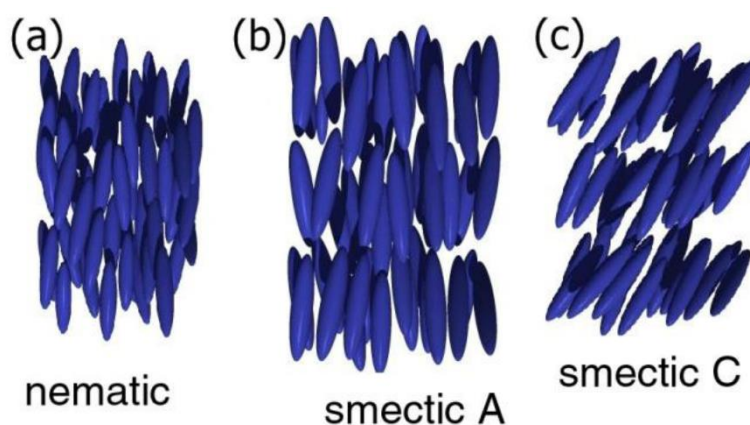


**Figure 1.** A different view of the mesophase structure. The orientation of the molecular director is represented by the arrows: a) nematic, b) smectic A, c) smectic C [5]

For flow analysis the microencapsulated or used of thermochromic slurries of liquid crystals can be used to make visible the temperature and velocity fields in liquids. By dispersing the liquid crystal material into the liquid they become not only classical tracers used for flow visualisation but simultaneously small thermometers monitoring local fluid temperature [6]. The liquid crystals can be also used as temperature sensors in the case of investigations in strong magnetic field [7-8]. Magnetic field was the source of additional force, which was able to enhance heat transfer of paramagnetic fluids connected directly with temperature changes indicated by the liquid crystals. To get the qualitative information about temperature field an image analysis is necessary. Some publications described the suitability of color space transformations for such optical temperature measurements [9].

Before the execution of a thermal mapping or flow visualization experiment, we should recognize the characteristics of the overall combination of TLC, the light source, the optical camera system (ordinary, CCD black and white or RGB camera), and make a rational plan for the total measurement system. The relationship between the temperature of the crystal and the measured Hue (in the HSI – hue, saturation, intensity) of the reflected lights defines the calibration curve for the liquid crystal. The result is a curve relating the Hue of the reflected light to the surface temperature. A known temperature distribution exists on a ‘calibration plate’ (brass plate) to which is attached the liquid crystal layer. In order to maintain a linear temperature distribution with desired temperature gradients, one end of a brass plate was cooled by stabilized water and the other end controlled electrically to give a constant temperature [10-11]. The brass plate with the liquid crystal layer is calibrated in place in the wind tunnel with the same lighting level and viewing angle used during the data acquisition phase of the experiment [11]. The distribution of the colour component pattern on the liquid crystal layer was measured by RGB colour camera and series of images at a different temperatures defines the calibration.

Two main methods of surface temperature measurement are performed involving steady state and transient techniques which requires measurement of the elapsed time to increase the surface temperature of TLC-coated test specimen from a known initial temperature predetermined value [12-13].

Liquid crystals can be also used to make visible temperature and velocity fields in liquid by the simple expedient of directly mixing the liquid crystal material into the liquid in the small quantities. As opposed to all of the preceding researchers, who used encapsulated liquid crystals the team of Kowalewski and Stasiak [6] dissolved encapsulated chiral-nematic material in ether and sprayed the mixture into the air above a free-surface of glycerol. The ether evaporated in mid-air, leaving small drops of liquid crystal material which fell into the glycerol forming an ‘almost mono-dispersed’ suspensions of particles approximately 50 microns in diameters or less. The concentration was kept below 0.02 % by weight.

### 3. Particle Image Velocimetry

Particle Image Velocimetry technique is another well-established experimental method in fluid mechanics, that allows quantitative measurement of two-dimensional flow structure. More recently, this technique has been applied to study of heat and fluid flow in complex geometries with highly non-uniform boundary conditions [14-19].

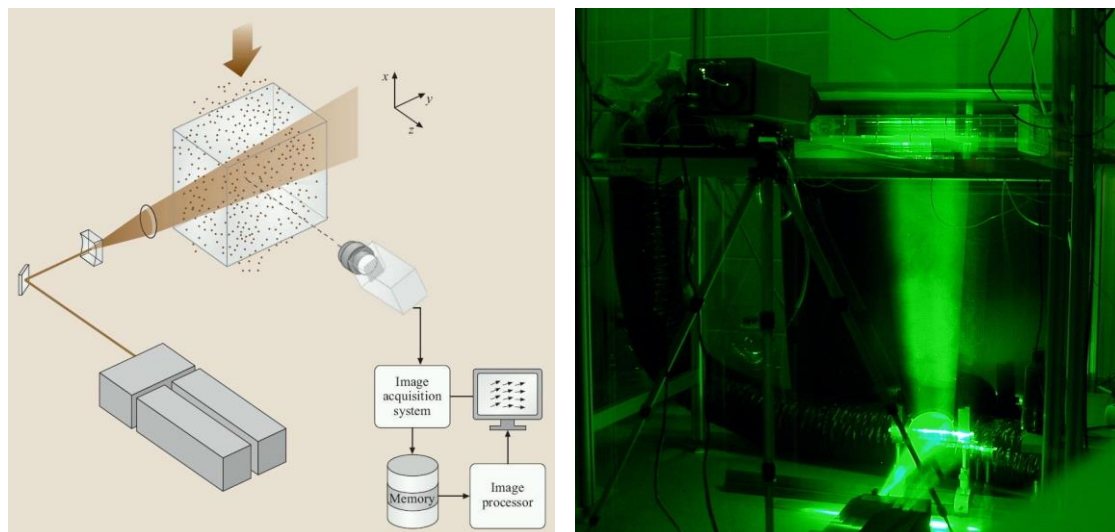


**Figure 2.** Schematic of a typical PIV measurements (left) and “laser light sheet” (right)

It enables measurements of the instantaneous in-plane velocity vector field within a planar section of the flow field and allows to calculate spatial gradients, dissipation of turbulent energy, spatial

correlations, and the like. In PIV technique selected cross-section of the investigated seeded flow is illuminated by laser light formed in thin “light sheet” (figure 2). Images of the flow are recorded by CCD camera and correlated to calculate instantaneous velocity fields. At presents the PIV measurements were performed for pure air seeded with small droplets (few micrometers in diameter) of synthetic oil DEHS (Di-Ethyl-Heksyl-Sebacat). The oil drops volumetric concentration was very low hence they did not affect the flow structure.

#### 4. IR-Photography

Infrared photography is a non-contact measurement method, which enables visualisation and registration of temperature distribution on the surface. Every object with temperature above 0 K emits radiation as an electromagnetic wave. Radiation in the range of  $0.8 \mu\text{m}$  up to  $1000 \mu\text{m}$  is non visible by human eye and is called infrared radiation (IR). Its intensity is a function of temperature and emissivity of the object surface. IR-photography measures from the distance intensity of infrared radiation emitted by the body and converts it into digital signal. That signal is enhanced and transformed, which leads to obtaining a temperature field of measured object as a thermogram (map of temperature field). It can be later analysed using computer software. This technique has wide applications in industrial [20-21], scientific [22-24] and medical thermography [25].

#### 5. Experimental facility for heat and flow visualisation

The experimental study was carried out using an open low-speed wind tunnel consisting of entrance section with fan and heaters, large settling chambers with diffusing screen and honeycomb, and then working sections (figure 3).

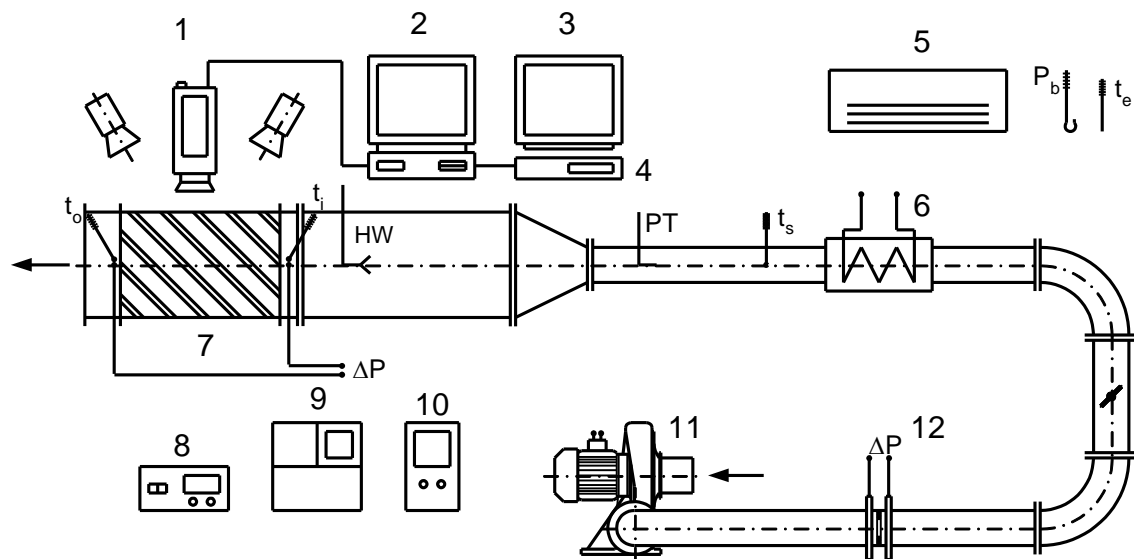


**Figure 3.** Open low speed wind tunnel, 1 – RGB camera (TK-1070), 2 – PC, 3 – monitor (RGB-VMR 200), 4 – S-VHS recorder, 5 – air conditioning system, 6 – heater, 7 – LC mapping section, 8 – digital micro manometer FCO 12, 9 – DISA hot wire system, 10 – variac, 11 – fan, 12 – orifice

Air is drawn through the tunnel using a fan able to attain the Reynolds numbers in the range from 500 to 40 000. Local and mean velocity are measured using conventional Pitot tubes and DISA hot-wire velocity probe. The liquid crystals used here, manufactured in sheet form by Hallcrest [26], had an event temperature range from  $30.0$  to  $35.0^\circ\text{C}$ . In this particular experiment uncertainty for temperature measurement was estimated at about  $\pm 0,05^\circ\text{C}$  by considering only the section of the surface used in the experiment, span-wise non-uniformities in Hue value are minimized.

In many cases, as mentioned above, remarkable enhancement of local and spatially averaged surface heat transfer rates are possible with rib turbulators, in spite of the lower local Nusselt number at certain

locations along the ribbed surfaces. The test surface that is analyzed contains a collection of rib turbulators that are perpendicular and angled with respect to the flow stream (figure 4) [27].

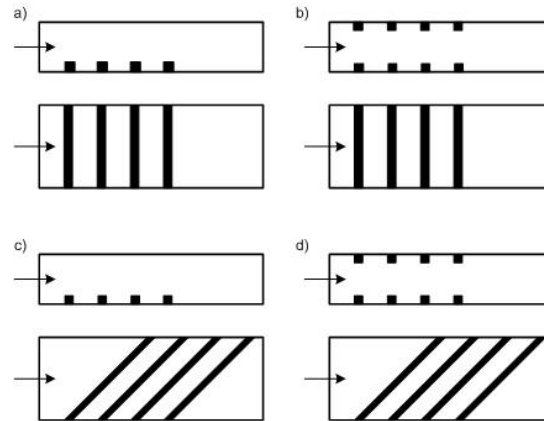


**Figure 4.** Schematic view of four types of transverse vortex generators (rectangular ribs)

To determine the surface heat flux (used to calculate heat transfer coefficients and Nusselt numbers), the convective power levels provided by the thermofoil heaters are divided by flat test surface area. Spatially resolved temperature distributions along the bottom rib turbulator test surface are determined using liquid crystals thermography (LCT) and true-color image processing system commercially available from Hallcrest [26]. Experimental facility is also equipped with Infrared Camera FLIR T440bx. T-Series camera offer superior sensitivity, high resolutions, excellent infrared image quality and reliable temperature measurement accuracy at an affordable price, which is ideal for scientific applications. FLIR T440bx has been specifically designed to have 8 times continuous digital zoom with a temperature range from  $-20^{\circ}\text{C}$  to  $1200^{\circ}\text{C}$ , MSX Thermal Image Enhancement and many other features.

## 6. Examples of experimental results

In the following examples the TLC's plastic sheet and capsulated TLC's tracers have been applied to measure both temperature and velocity flow fields. For human body screening or biomedical situations few images using TLC and IR-Photography techniques are also presented.

### 6.1. Full field surface temperature measurements

Liquid crystals can be used to determine the distribution of the surface temperature, and if the surface heat flux can be found, this allows evaluation of the heat transfer coefficient or the Nusselt number.

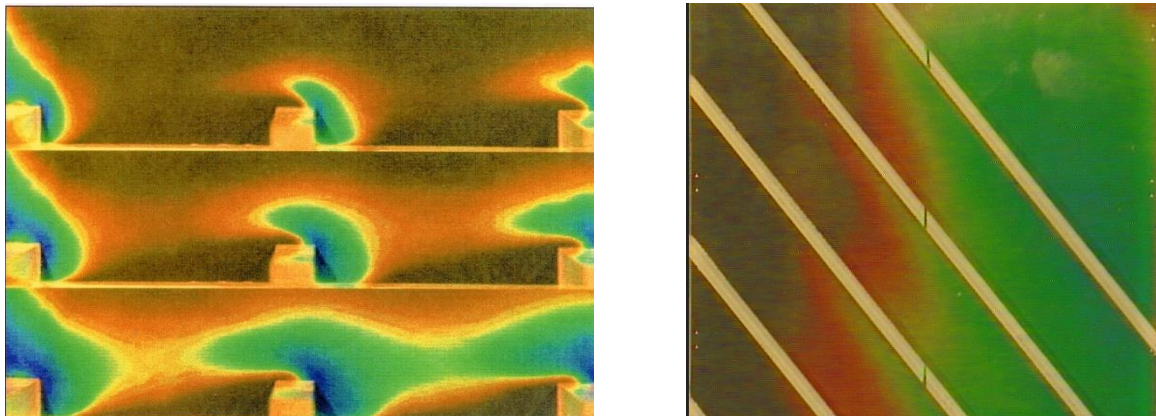


**Figure 5.** True-colour image from TLC for an endwall surface with columns (left) and visualization of model heat exchanger with vortex generators: ribbed surface - true-colour image (right)

Left image in figure 5 shows photographs of the colour distribution of the liquid crystal layer around a square section column.

Improvements in flow and thermal characteristics of heat exchanger do not require any demonstrations and would substantially reduce fuel and production costs. The measuring technique comprising the use of LC flexible sheets and true-colour processing may also be used for a great variety of applications and should be of considerable use in improving the design of all types of compact heat exchanger. Experimental procedures cover full field flow patterns in classic heat exchanger elements (flat plate with fine-tubes in-line, staggered and with vortex generators) describing local heat transfer coefficient and Nusselt number on the surfaces. An examples of such results are presented on right image in figure 5.

Nusselt number distribution for channel with vortex generators (rib turbulators) for one geometry with ribbed bottom and top walls (geometry b in figure 4) for different Reynolds numbers (9,000; 16,000; 26,000; 35,500) in the boundary layer is shown in figure 6. The analysis of the boundary layer was carried out to assess the impact of the channel wall on heat transfer. More information can be found in [27].

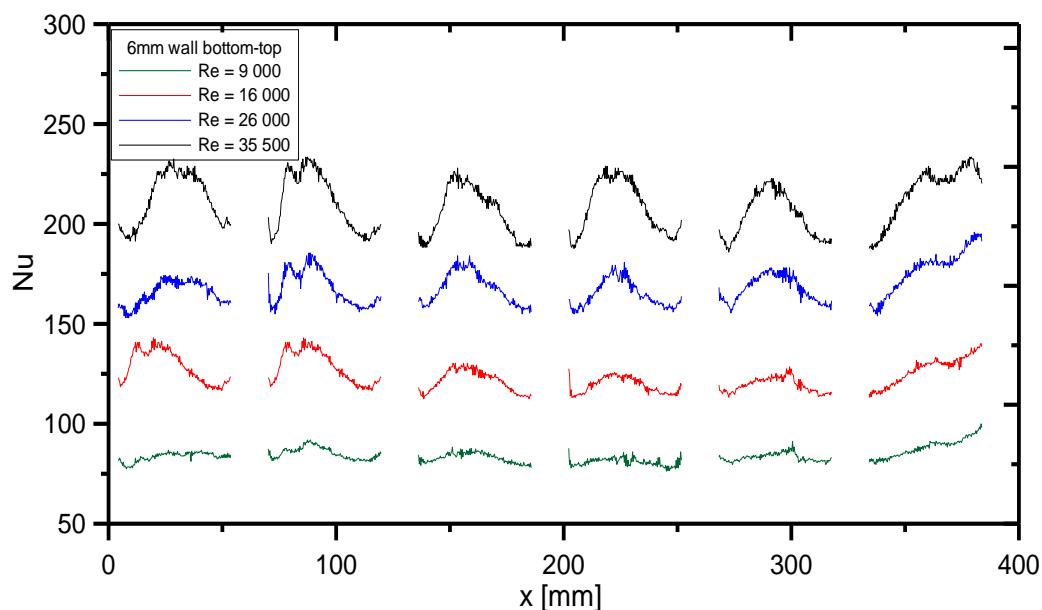


**Figure 6.** Local streamwise Nusselt number distribution between ribs in a boundary layer for ribbed bottom and top walls and ribs perpendicular to the flow

### 6.2. Natural convection in a closed cavity

Vertical temperature gradients are mainly responsible for the atmospheric or oceanographic fluid motion. Development of the nocturnal stable stratification over flat areas, inversion of temperature gradient and break-up of the convective boundary layer developed at the ground levels can be simulated using small-scale laboratory experiments.

One of the typical features characterizing instabilities generated by vertical temperature gradient are plumes or ejections appearing, when the thermal boundary layer breaks up. Figure 7 shows temperature and velocity visualization in glycerol-filled cavity under free convection in horizontal and vertical position. The photographs were made perpendicular to the line of the illumination. The specimen was illuminated using Xenon flash lamp collimated by a cylindrical lens to form a sheet which could be adjusted by 1 to 2 mm in width. The flashing of lamp was controlled by computer to flash with specified intervals between flashes from 3 seconds to 60 seconds.

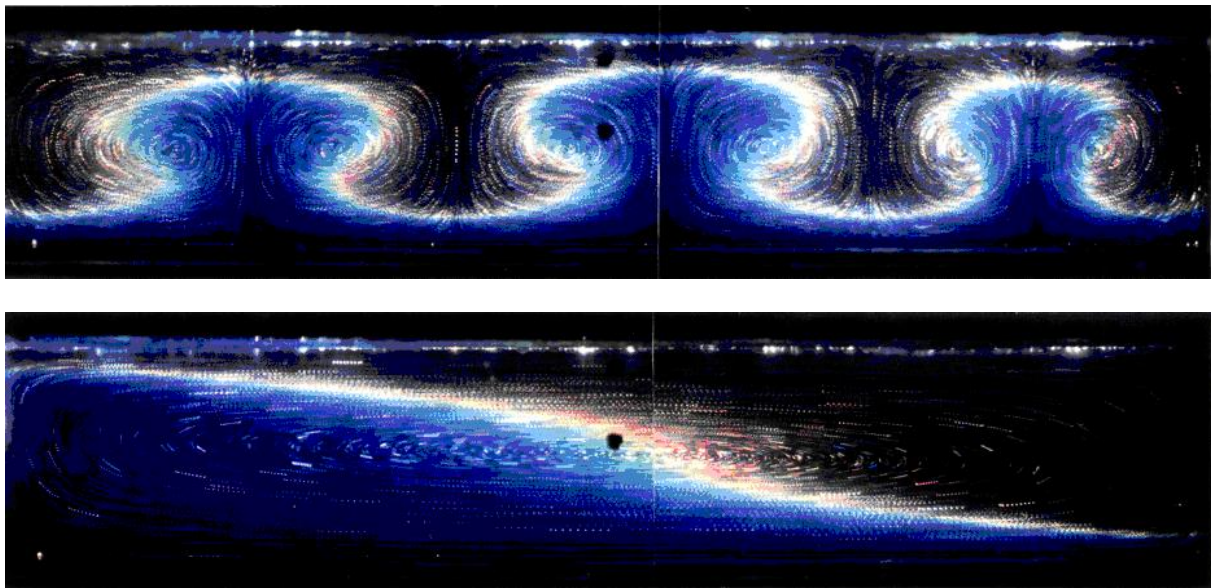


**Figure 7.** Visualisation of Benard cells in the horizontal (top) and vertical (bottom) cavity using TLC

### 6.3. Visualization of film cooling of model turbine blades

Internal cooling technique for gas turbine blades has been studied for many years. The designers need detailed data for heat transfer and temperature distributions along with the flow and streamwise pressure gradient to understand the flow physics and to improve the current internal cooling designs. Examples of modified gas turbine blades are shown in figure 8, left side [28]. Within this objective, TLC technique also has been applied to study of aerodynamic and aerothermal blade turbine design with effusive cooling concept. View of test section of low-speed wind tunnel is presented in figure 8, right side. Examples of steady-state and transient LCT measurements and visualization are shown in figure 9.



**Figure 8.** Gas turbine blades with cooling holes (left) and view of test section for model turbine blade cooling (right)



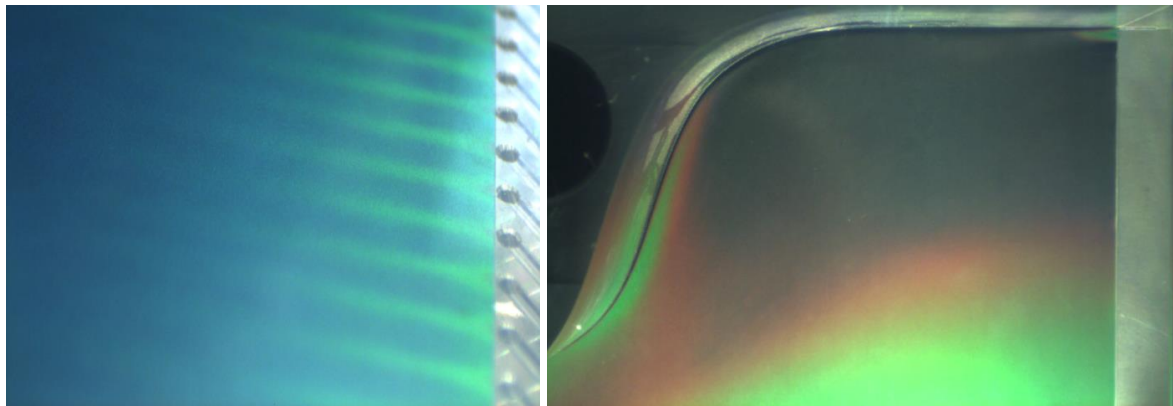


**Figure 9.** Steady-state LTC visualization of air flow on a blade surface with air jets (left) and end-wall temperature distribution by transient TLC method (right)

#### 6.4. PIV measurements

Velocity fields in case of ribbed channel were obtained from the PIV measurements for different ribs geometries (figure 4) and different Reynolds numbers ( $Re = 9000, 16,000$  and  $26,000$ ). The area scanned by the PIV method was in all cases located in the mid-vertical-plane between side walls (one position of the laser light sheet).

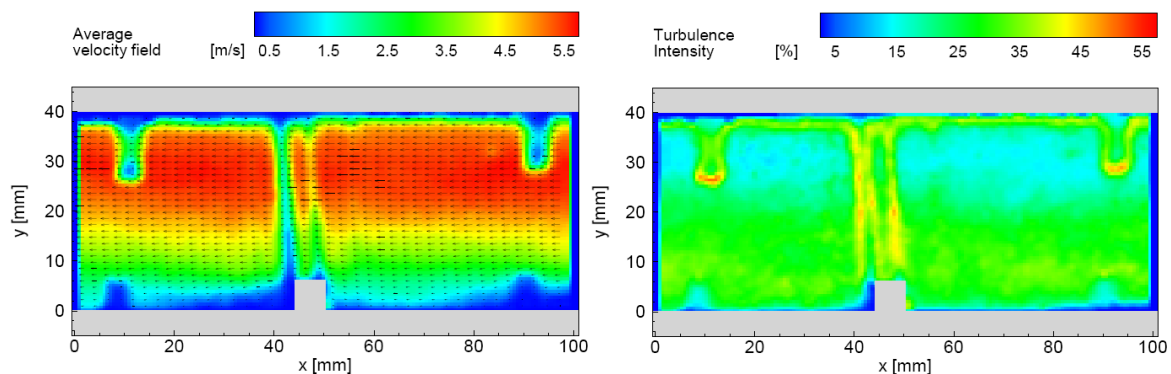


**Figure 10.** PIV measurements for ribbed channel: averaged velocity field (left) and turbulence intensity (right) for geometry with ribbed bottom wall

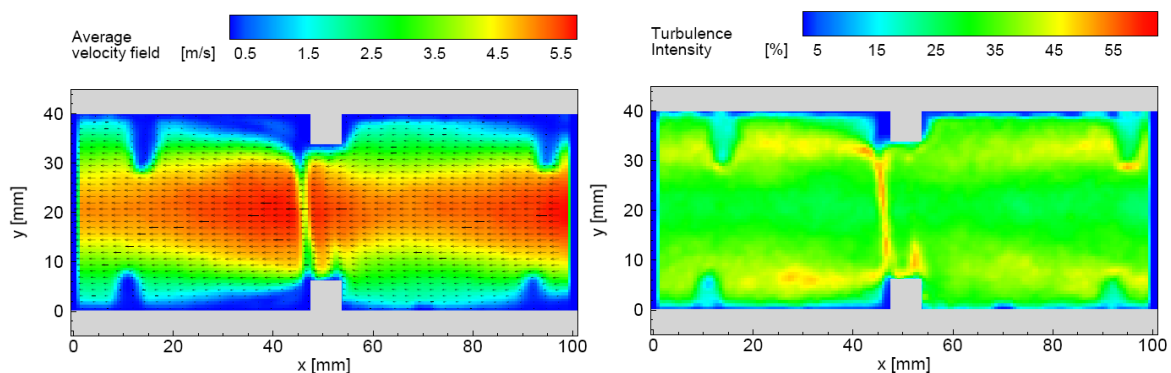


**Figure 11.** PIV measurements for ribbed channel: averaged velocity field (left) and turbulence intensity (right) for geometry with ribbed bottom and top walls

Figure 10 shows an average velocity field (averaged over 100 instantaneous velocity fields) for a geometry with ribbed bottom wall only (ribs height is 6 mm) and flow perpendicular to the ribs

((geometry a in figure 4)), while figure 11 show geometry with ribbed top and bottom walls (geometry b in figure 4). Reynolds number is 16,000. Maximum velocity for this cases is about 5.5 m/s and is located in the top part of the channel. Figures 10-11 show also a turbulence intensity computed from 100 instantaneous velocity fields.

### 6.5. Medical applications

Both, liquid crystal thermography and infrared photography, as non-invasive diagnostic techniques, can be used for skin surface temperature measurements. Obtained images can give information about pathological phenomena in the patient organism.

Liquid crystals in the mode of thermographic examination, can be also used in the case of diagnostics and monitoring of different diseases e.g.: diagnosis of cancers, tumours and inflammatory states (liver, lung, etc.), evolution of skin tests (allergy, tuberculin), traumatology and forensic medicine. Those methods are especially useful for children because they are non-invasive, fast, reliable and visually attractive. Because the temperature of human skin depends upon the metabolic level of neighbouring tissues, heat transfer can occur via muscular and adipose tissues, blood circulation, muscular tensions, body position or effect of drugs. This kind of medical diagnosis should be confirmed by other independent methods in the case of diseases suspicion [13].

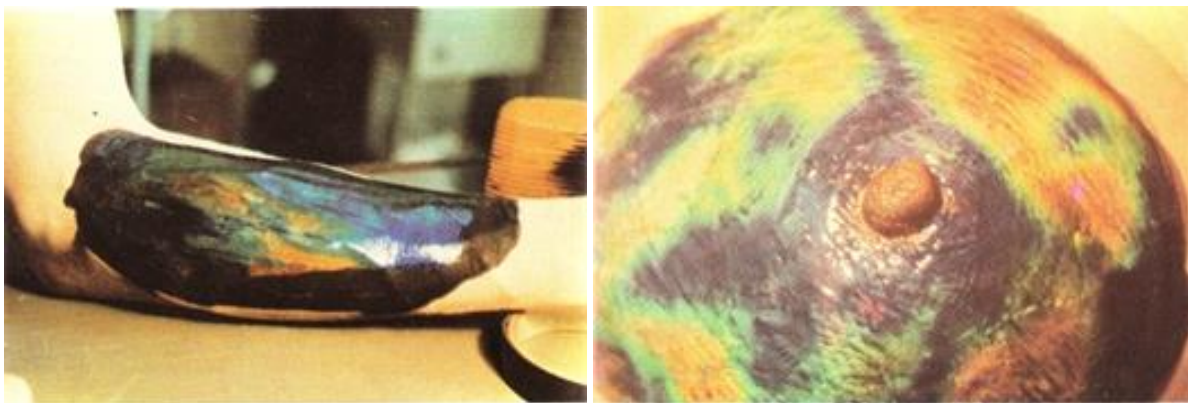


**Figure 12.** LC thermogram of forearm (left) and breast cancer (dark region) (right)

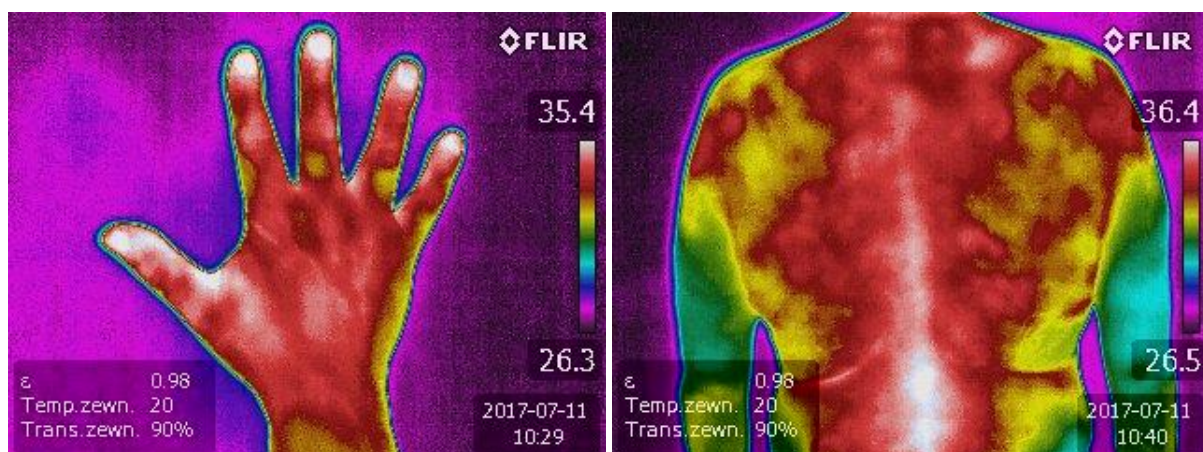


**Figure 13.** IR thermogram of human hand and human back

Requirements for thermographic examination are well-known [29]. The minimum area of a testing room has to be 9 square metres. All devices emitting heat should be removed, if possible. Air movements have to be minimised. The preferred temperature of the testing room should be 25 to 27°C, while

humidity should be 50 to 70 %. Both these parameters should be carefully controlled during measurement. The effect of sunlight should be minimised. Light sources have to secure scattered light of low intensity to avoid light reflections. Patients should abstain from physical activity during 20 minutes before measurement. The skin area studied should be exposed for at least 15 minutes before a test to ensure thermal equilibrium with the environment [13].

The patient's position should be similar to their physiological (normal) one to avoid temperature changes due to enforced changes of blood circulation. Body areas studied should not contact other body areas. Medicines, drugs (alcohol, nicotine and so on) and treatments affecting blood circulation should not be taken, if possible, for 24 hours before measurement. Also patients should not have cold and hot drinks and not eat large meals before measurement. Cosmetics can also affect thermal properties of skin. All subsequent measurements have to be done at the same hour of the day. The thermological report should contain all conditions of measurement, including the states of the patient and environment. The patient should be allowed to see the thermographic images because their colours have a positive psychological effect especially in the case of children. Various cases have been studied and typical results of LCT are shown in figure 12 [29], while figure 13 shows examples of infrared images of a human body taken by FLIR T440bx camera.

## 7. Conclusions

Advanced experimental techniques, in this case true-colour image processing of liquid crystal patterns, particle image velocimetry and infrared imaging, allow new approaches to old problems and open up new areas of research and applications. Image processing data make available quantitative, full field information about the distribution of temperature, heat transfer and adjunctive medical pathogenesis and diagnostics. It is evidence from our research that liquid crystal and infrared imaging technique have many applications, not only in testing, but also in industry, medicine and the home.

The presented overview provides an introduction to thermochromic liquid crystals, digital infrared imaging and particle image velocimetry, how this measurements techniques and methods work and how they are used.

## References

- [1] Reinitzer R, 1899 *Monatschr, Chem, Wien* 9 pp 421-441
- [2] Moffat R J, 1991 *Proc. 9<sup>th</sup> Intl. Heat Transfer Conference* Jerusalem Vol. 1 pp 308-310
- [3] Jones T V, Wang Z, Ireland P T, 1992 *Proc. Of the First I.Mech.E. Seminar on optical methods and Data Processing in Heat and Fluid Flow* City University London pp 51-65
- [4] Stasiak J, 1997 *Heat and Mass Transfer* 33 pp 27-39
- [5] Dierking I, 2014 *Chiral Liquid Crystals: Structures, Phases, Effects, Symmetry* 6(2), 444-472
- [6] Stasiak J A and Kowalewski T A, 2002 *Optoelectronics Review* 10 No.1 pp 1-10
- [7] Fornalik E, Filar P, Tagawa T, Ozoe H and Szmyd J S, 2006 *Intl Journal of Heat and Mass Transfer* 49 pp. 2642-2651
- [8] Fornalik E, 2007 *Journal of Theoretical and Applied Mechanics* 45 pp 557-568
- [9] Ziemia A and Fornalik E, 2016 *Journal of Physics Conference Series* 745 032108
- [10] Akino N, Kunugi T, Ichimiya K, Mitsuchiro K and Ueda M, 1989 *ASME J.Heat Transfer* 111 pp 558-565
- [11] Stasiak J, Collins M W, 1996 *Atlas of Visualization* Vol 2 CRC Press Inc USA
- [12] Stasiak J, Jewartowski M and Kowalewski T A, 2014 *Journal of Crystalization Process and Technology* 4 pp 46-59
- [13] Stasiak J, Stasiak A, Jewartowski M and Collins M W, 2006 *Optics & Laser Technology* 38 pp 243-256
- [14] Ambrosini D, Paoletti D, Galli G, 2015 *World Congress on Mechanical, Chemical and Material Engineering* Barcelona, Spain 325
- [15] De Leo C, Paoletti D, Ambrosini D, 2018 *The European Physical Journal Applied Physics* 82(3) 30501

- [16] Lindken R, Gui L, Merzkirch W, 1999 *Chemical Engineering and Technology* 22(3) pp 202-206
- [17] Adrian R J, 2015 *Experiments in Fluids* 39(2) pp 159–169
- [18] Merzkirch W, 2018 *Particle Image Velocimetry. In: Optical Measurements* pp 341-357 Springer, Berlin, Heidelberg
- [19] Stabile L, Arpino F, Buonanno G, Russi A, Frattolillo A, 2015 *Building and Environment* 93 pp 186-198
- [20] Bagavathiappan S, Lahiri B B, Saravanan T, Philip J and Jayakumar T, 2013 *Infrared Physics & Technology* 60 pp 35-55
- [21] Nardi I, Lucchi E, de Rubeis T, Ambrosini D 2018 *Building and Environment* 146 pp 190-205
- [22] Mikielewicz D, Wajs J, Glinski M and Zrooga A-B R S, 2013 *Experimental Thermal and Fluid Science* 44 pp 556-564
- [23] Wajs J, Mikielewicz D, 2017 *Archives of Thermodynamics* 38(1) pp 123-139
- [24] Raiola M, Greco C S, Contino M, Discetti S, Ianiro A, 2017 *International Journal of Heat and Mass Transfer* 108, 199-209
- [25] Polidori G, Renard Y, Lorimier S, Pron H, Derrau S and Taiar R, 2017 *Int. Journal of Surgery Case Reports* 34 pp 56-59
- [26] HALLCREST, 2014 *Handbook of Thermochromic Liquid Crystal Technology* LCR Hallcrest
- [27] Mikielewicz D, Stasiek A, Jewartowski M and Stasiek J, 2012 *Applied Thermal Engineering* 49 pp 61-72
- [28] Giampaolo A, 2006 *Gas turbine handbook: principles and practices* The Fairmont Press, Inc.
- [29] Zmija J, Klosowicz S and Borys S, 1989 *Cholesteric liquid crystals in a detection of radiation* (Warsaw: Poland/WNT in Polish)